

Laryngeal Nerve Identification during Thyroid Surgery with Automatic Adjustment of Electrical Signal Parameters

MYKOLA DYVAK, VOLODYMYR TYMETS, ANDRIY DYVAK

Department of Computer Science, West Ukrainian National University, Ternopil, Ukraine

Corresponding author: Mykola Dyvak (e-mail: mdy@wunu.edu.ua).

ABSTRACT The article presents the results of developing the method and tools for localization and visualization of the recurrent laryngeal nerve (RLN). It is based on an electrophysiological method of tissue surgical wound stimulation with software adjustment of the electrical signal parameters to achieve a maximum response of the vocal cords depending on the electrophysiological properties of the surgical wound tissue. The reaction to tissue stimulation is recorded by a sound sensor, and subsequent processing of the received information signal is done by a computer based on a Raspberry Pi 4 single-board computer. The results of processing are visualized by a portable display indicating the area on the surgical wound with the greatest risk of possible damage to the RLN. The time characteristics of each of the stages of obtaining an information signal, setting the parameters of the electrical signal, and visualizing the results of the detection of the RLN are studied. Optimization of the specified time characteristics provides a response to stimulation during a single inhale or exhale of the patient during surgery. The article also proposes a method for building an interval model of the distribution of information signal characteristics, which determines the properties and type of tissue on a surgical wound and, accordingly, makes it possible to build the area of the highest risk of damage to the RLN. The mentioned method is based on the analysis of interval data and the iterative procedure of refining the model every time the surgeon stimulates the tissues of the surgical wound with an electric current. In total, the developed methods and tools provide a reduction in the time for the operation and reduce the risk of damage to the RLN as a result of visualization of its location on the surgical wound.

KEYWORDS algorithm and hardware; electrical signal; operations on neck organs; recurrent laryngeal nerve; electrical stimulation; intraoperative monitoring.

I. INTRODUCTION

Damaging of the RLN is one of the most dangerous consequences of thyroid surgery [1-3]. Therefore, during a surgical operation, continuous control (monitoring) of the functional ability of the RLN is carried out [4]. It is worth noting that a significant number of scientific publications on thyroid and parathyroid surgery have been devoted to this issue [5]. In particular, one of the most common ways to reduce the risk of damage to the RLN is neuromonitoring using a range of tools [6]. However, none of the existing tools in thyroid surgery protects the patient from possible negative consequences of this surgery. Recently, to reduce the risk of damage to the RLN, electrophysiological methods of stimulating the tissues of a surgical wound with an electric current are used, followed by an in-depth analysis of the result of the stimulation with the help of computer tools. The result of stimulation, in the form of a sound signal, is obtained from the vibration of the patient's

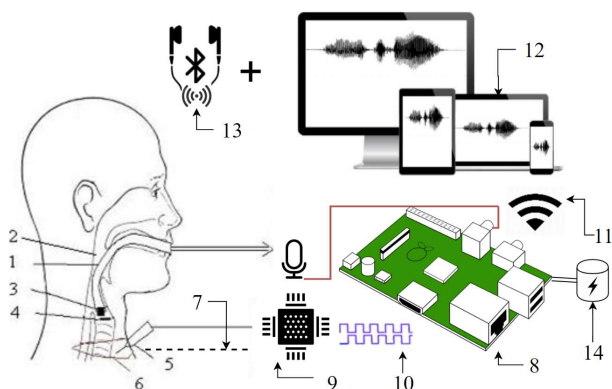
vocal cords as a result of the passage of an electrical signal through the RLN [7]. However, this approach also has disadvantages, since the larynx and arrangement of the vocal cords of each patient has its characteristics and, accordingly, the received acoustic signal will be different for each patient. On the other hand, the electrophysiological properties of the surgical environment are different for each patient [8]. In several papers [9, 10], it was suggested that part of the time required to detect the RLN should be spent on setting the parameters of the electrical signal and on building a model based on interval data analysis [11, 12] for tissue classification. However, such an approach requires the study of the time characteristics of each of the stages of receiving the information signal, setting the parameters of the electrical signal, and visualizing the results of the identification of the RLN. It is necessary to ensure the optimization of the specified time characteristics. This will make it possible to adjust the

signal parameters under constant conditions, namely during a single inhalation or exhalation of the patient. As a result, the efficiency of identification of RLN increases and the time for surgical operation is reduced.

II. DESCRIPTION OF EXISTING SOFTWARE AND HARDWARE SOLUTION

Let us consider the principles of functioning of the existing software and hardware complex for the identification of RLN in the process of thyroid surgery. The main functional components of the device are shown in Fig. 1 [9].

The respiratory tube (1) with the sound sensor (3) was installed in such a way that the sensor was located above the vocal cords (4). The active electrode (5) is connected to an electric current generator (9). The single-board computer (8) is controlled by this generator. With the help of an active electrode (5), the tissues of the surgical wound (6) are stimulated with an electric current in the form of rectangular pulses. As a result, the vocal cords (4) stretch, due to the contraction of the muscles that control them. The flow of air passes through the patient's larynx and is modulated by vibrated vocal cords. The resulting sound is recorded by the sound sensor (3) and through the sound adapter is transmitted to the single-board computer (8) for processing. The results of stimulation and signal processing are displayed using the visualization unit (12) and accompanied by sound informing the surgeon about the type of tissue (13).



1) respiratory tube; 2) larynx; 3) microphone; 4) vocal cords; 5) active probe; 6) surgical area; 7) passive probe; 8) main hardware part of the device (Raspberry Pi); 9) additional hardware part of the device (electrical current generator); 10) rectangular pulses.; 11) Wi-Fi - transfer information between devices; 12) visualization hardware part of the device (tablet, phone, personal copy, laptop); 13) Bluetooth headphones; 14) source of power

Figure 1. Functional diagram of the process of intraoperative neuromonitoring of laryngeal nerves during surgery on the thyroid gland [9].

As it can be seen, there is no function of adjusting the frequency tissue stimulation pulses of the surgical wound to adjust it to the electrophysiological characteristics of the tissues of the patient's surgical wound in traditional architecture. The specified function is implemented in the next version of the device, which is built on the basis of a single-board computer based on Raspberry Pi-4.

III. ALGORITHM OF ADAPTIVE ADJUSTMENTS

Let us consider how the new version of the device is based on Raspberry Pi-4 functions. The well-known technology for detecting the location of RLN involves five steps.

Step 1. Stimulation of tissues of a surgical wound with a

pulsed electrical signal of a fixed frequency.

Using the newly developed device, in contrast to existing technologies [13, 14], the tissues of the surgical wound are stimulated with pulsed electric current at frequencies from 2 to 20 Hz. At the same time, we fix the current strength in the range from 0.5 mA to 2 mA.

Step 2. Obtaining of information signal (as result of stimulation of surgery wound tissues)

Since in the known method, the result of stimulation is recorded using a microphone installed in the endotracheal tube, the received audio signal is fed to the audio adapter, where it is digitized and fed to the Raspberry Pi 4 single-board computer for processing.

All software is implemented based on a Raspberry Pi 4 single-board computer. It controls all other devices, including the rectangular pulse generator, as well as processing the received audio signal and visualization of the processing and classification of the tissue of the surgical wound at the point of stimulation.

Step 3. Information signal segmentation software.

This is a standard step implemented in the device in Fig. 1. It also applies to existing methods of identifying the location of the RLN. The current step is needed to highlight the patient's reaction to tissue stimulation from sound signals taken during inhale or exhale.

In Fig. 2, the information signal is displayed and the segmentation principle is visually represented. There are two types of segments. Segments of the first type are the result of the propagation on the RLN of the effect of each impulse on the muscles that stretch the vocal cords. There are four such segments in Fig. 2. Segments of the second type reflect the intervals between stimulation signals and represent the sounds produced by a patient during a single inhalation or exhalation. Other intervals are intervals between the segments of a patient's breath. It is necessary to select type 1 segments, as shown in Fig. 2, during the segmentation process.

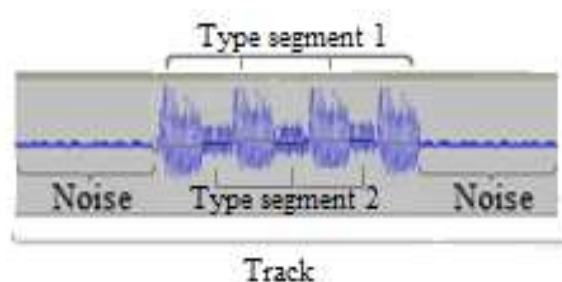


Figure 2. Illustration of the information signal segmentation.

Representing the audio signal digitally simplifies segmentation and enables programmatic processing using Raspberry Pi 4. For this, the threshold method of determining the beginning and end of the fragment is used [9].

Step 4. Selecting of the main spectral component.

In practical applications of the method of identifying the location of the RLN considered above, the values of the average count amplitude on segments of type 1 and 2 are used (see Fig. 2). However, this approach often leads to false classification of tissues, since the result also depends on the strength of the stimulation current. Therefore, in later works [15] regarding the implementation of this method, it is proposed to use the amplitude of the main (with the maximum amplitude) spectral component of the signal segment to classify

tissues at the point of stimulation. This can be achieved using the fast Fourier transform [16-18].

Step 5. Classification of tissues and result visualization.

Work [9] shows that the amplitude of the main spectral component of the information signal directly depends on the distance between the point of stimulation on the surgical wound and the RLN. This regularity is the basis of the algorithm for classifying surgical wound tissues. The greater the amplitude of the main spectral component, the closer the tissue stimulation point is to the RLN and vice versa.

In this way, the process of identification of the RLN in the known solution was carried out in five steps.

The main drawback of the proposed solutions is the lack of procedures for adjusting the frequency of the generated pulses, which does not provide automatic adjustment of the parameters of the electrical signal to stimulate the tissues of the surgical wound in the most effective way.

Therefore, the authors add one more step to the algorithm described above, which provides this automatic setting. It should be noted that this step is used only at the beginning of the monitoring procedure.

Step 6. Setting up the parameters of the electrical signal to stimulate the surgical wound tissues.

As mentioned above, the efficiency of the response to wound tissue stimulation depends on the frequency of the impulse electric current. As indicated above, we will choose typical frequency values for electrical stimulation in the range of 2 Hz to 20 Hz. This range is determined by the limits of the possible reaction of muscle tissues to electrical impulses. To adjust this parameter of the stimulation signal to optimal values, a loop is set between the stimulation frequency and the result evaluation in the form of the calculated amplitude of the main spectral component at three points of the surgical wound: around the RLN - at a distance of 2-3 mm; at a distance of more than 1 cm from the RLN. The algorithm for each point is as follows.

Step 6.1. Setting the pulse current frequency value to 2 Hz.

Proceeding to step 1.

Step 6.2. Implementation of steps 1-5.

In this case, the result is the amplitude of the main spectral component.

Let us define it as $A_b(f)$, where f - the frequency of the stimulation impulse current.

Step 6.3. Verification:

$$\text{If } A_b(f) > A \text{ then } A := A_b(f); f_{opt} := f, \quad (1)$$

$$\text{If } f < 20 \text{ then } f := f + 1 \text{ and proceeding to step 1,} \\ \text{else save } f_{opt} \text{ and stop step 6.} \quad (2)$$

It is worth mentioning that the meaning of the symbol := in step 6.3. is to assign, and the expression “save f_{opt} and stop step 6” means that this step is no longer used in the process of calculations and RLN monitoring, and the f_{opt} stimulation frequency remains unchanged.

In this way, the proposed algorithm solves the problem of setting the parameters of the electric signal for the stimulation of the RLN. As already mentioned, for its implementation, it is necessary to change the hardware, namely the single-board computer to a newer version with higher performance.

However, in any case, there are certain problems with the use of the proposed method of solving the problem of effective stimulation of surgical wound tissues. First of all, this concerns

the method of setting up the process of finding the effective frequency of the pulse signal stimulation. A simple (linear) frequency sweep of the electrical signal from 2 Hz to 20 Hz requires 19 cycles during which the tissues of the surgical wound should be constantly stimulated. At the same time, the procedure for adjusting the stimulation frequency should be performed only during the same inhalation or exhalation of the patient. Therefore, in practice, the proposed method of adjusting the parameters of the electrical stimulation signal turned out to be ineffective.

IV. ANALYSIS OF TIME ASPECTS OF THE IMPLEMENTATION OF THE METHOD OF ADJUSTING ELECTRICAL SIGNAL PARAMETERS

As it is known, respiratory rate for a healthy adult is 12–15 breaths per minute in normal conditions [19, 20]. Which is an average of 2 seconds per inhalation and exhalation.

To confirm the above, the breathing records of a sample of patients were analyzed. Fig. 3 shows samples of the received audio signals obtained during the breathing of three patients.

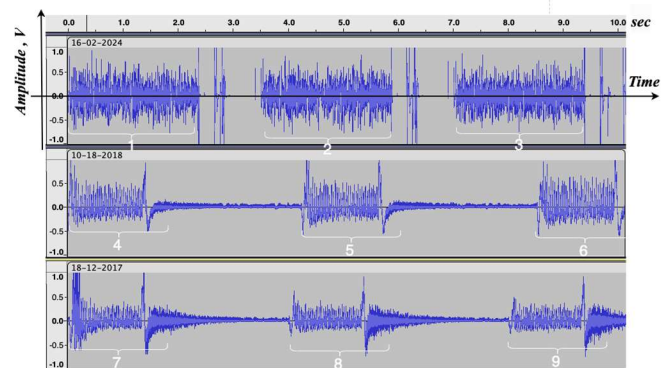


Figure 3. Samples of sound signals obtained by the sound sensor installed in the respiratory tube.

To determine the exact duration of each individual breath, software tools were used that showed the duration of each fragment in milliseconds. The results of the research are shown in Table 1.

Table 1. Duration of breath fragments for a sample of patients

N - fragments	Ms
1	2415
2	2390
3	2426
4	1840
5	1715
6	1815
7	2070
8	2043
9	2110
Average duration	2091,555556

As it can be seen, the average duration of one breath is **2091.555556 ms**, that is, about **2 seconds**.

As mentioned above, the frequency range of the electrical pulse signal that stimulates the tissues of the surgical wound is from 1 to 20 Hz. According to the algorithm proposed in article [9], in order to find the optimal frequency of stimulation using

the sorting method, it is necessary to stimulate the tissues of the surgical wound with all possible values from the appropriate range. Thus, to carry out this complete search, the time $t_{stimulation}$ spent only on the stimulation of the tissues of the surgical wound is equal to **3597 ms**. This is approximately equal to the duration of two inhalations (exhalations) of the patient, which makes it impossible to apply the algorithm given in Section II.

Moreover, in the process of identification of RLN, additional calculations are carried out at each of the 5 steps of the algorithm, which requires some processor time. Thus, the total time for examination of one point on a surgical wound using the above-described means increases. Fig. 4 illustrates the method of calculating the duration of the examination of one point on a surgical wound.

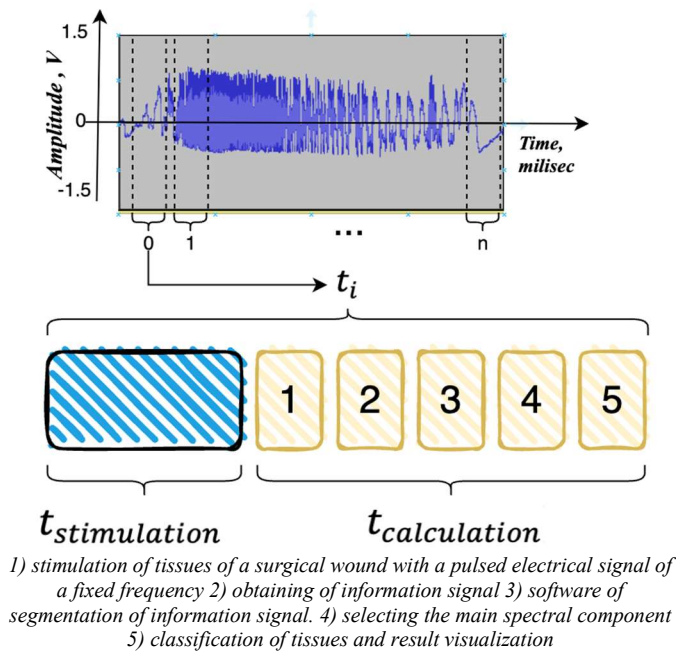


Figure 4. Illustration for calculating the examination time of one point on a surgical wound.

Table 2 shows the results of the research on time costs for each iteration of the algorithm using a single-board computer Raspberry Pi 4b.

Table 2. Time of operation of the algorithm of identification of the RLN on the Raspberry Pi 4b processor.

N	Name of Step	$t_{calculation}$ Ms
1	Stimulation of tissues of a surgical wound with a pulsed electrical signal of a fixed frequency.	0,125
2	Obtaining of information signal (as result of stimulation of surgery wound tissues)	12
3	Software of segmentation of information signal.	0
4	Selecting of the main spectral component	2,9
5	Classification of tissues and result visualization	0,001
	$t_{calculation}$	15,02

Based on Table 2, the duration of the processing the result of the reaction to the stimulation of the tissues of the surgical wound is calculated, taking into account the duration of the

stimulation:

$$t_i = t_{stimulation} + t_{calculation}i. \quad (3)$$

The results of calculations of the total time spent on the examination of one point on the surgical wound, which is associated with delays in the functioning of the electrical and electronic part of the device, are shown in Table 3.

Table 3. Time to determine the optimal stimulation frequency in the range from 1 to 20 Hz by the method of sorting through all possible values

Hz	$t_{stimulation}$ Ms	$t_{calculation}$ Ms	t_i Ms
1	1000	15,02	1015,0266667
2	500	15,02	515,0266667
3	333,3333333	15,02	348,36
4	250	15,02	265,0266667
5	200	15,02	215,0266667
6	166,6666667	15,02	181,6933333
7	142,8571429	15,02	157,8838095
8	125	15,02	140,0266667
9	111,1111111	15,02	126,1377778
10	100	15,02	115,0266667
11	90,90909091	15,02	105,9357576
12	83,33333333	15,02	98,36
13	76,92307692	15,02	91,94974359
14	71,42857143	15,02	86,4552381
15	66,66666667	15,02	81,69333333
16	62,5	15,02	77,52666667
17	58,82352941	15,02	73,85019608
18	55,55555556	15,02	70,58222222
19	52,63157895	15,02	67,65824561
20	50	15,02	65,02666667
Total	3597,739657		3612,766324

As it can be seen in Table 3, the total duration of the total time spent on examining one point on the surgical wound, which is associated with delays in the functioning of the electrical and electronic part of the device implemented in the known method, is unacceptable.

V. IMPROVEMENT OF ALGORITHM OF AUTOMATIC ADJUSTMENT OF THE ELECTRICAL SIGNAL PARAMETERS

To solve the above-mentioned problem of obtaining an effective stimulation frequency, additional research was carried out on various known algorithms, based on which it is possible to organize the optimal frequency selection of the electrical stimulation signal in the range from 1 to 20 Hz. This range is ordered by increasing frequencies, from the point of view of known sorting algorithms. Based on this, to improve the algorithm, several search algorithms in the sorted array can be applied.

Linear Search [21] – the use of linear search in the frequency determination algorithm means sequential stimulation of surgical wound tissues with all possible frequencies from 1 to 20 Hz. As mentioned above, the total duration of the time spent on examining one point on the surgical wound, in this case, is 3.6 seconds, which cannot allow us to find the optimal frequency of stimulation during one

inhalation.

Binary Search [22] – the application of this algorithm consists of dividing the frequency range in half and stimulating with an electrical signal with frequencies from the left and right diapason at each iteration. Table 4 shows the results of evaluating the total duration of the total time spent on examining one point on the surgical wound, which is associated with delays in the functioning of the electrical and electronic part of the device and in the case of applying the Binary Search algorithm in the sixth step.

Table 4. Time spent on examining one point on a surgical wound using Binary Search

N	Hz	Ms
1	5	215,0266667
2	15	81,69333333
3	3	348,36
4	7	215,0266667
5	2	515,0266667
6	4	265,0266667
		1640,16

As it is shown in Table 4, the time to find the optimal stimulation frequency using the Binary Search algorithm is 1.6 seconds. Thus, using Binary Search allows us to find the optimal frequency of stimulation during one inhalation (exhalation) by the patient.

Jump Search [23] – the algorithm combines elements of Binary and Linear search. Its implementation consists of applying a linear search with a certain step, and its reduction at each iteration. Table 5 below shows the duration of time spent on examining one point on a surgical wound, which is associated with delays in the functioning of the electrical and electronic part of the device, in case this algorithm is used to determine the optimal frequency of stimulation in the range from 1 to 20 Hz.

Table 5. Time spent on examining one point on a surgical wound using Jump Search

N	Hz	Ms
1	5	215,0266667
2	10	115,0266667
3	15	81,69333333
4	20	65,02666667
5	7	157,8838095
6	4	265,0266667
7	3	348,36
8	2	515,0266667
9	1	1015,026667
		2778,097143

As it can be seen in Table 5, the time to find the optimal stimulation frequency using Jump Search is more than 2.7 seconds. Thus, the use of Jump Search in step 6 does not allow for finding the optimal stimulation frequency during one inhalation (exhalation) by the patient.

Ternary Search [24] – the application of this approach consists in dividing the frequency range into 3 equal parts and stimulating the tissues with an electrical signal at the frequencies of each of these parts.

Table 6. Time spent on examining one point on a surgical wound using Ternary Search

N	Hz	Ms
1	3	348,36
2	9	126,1377778
3	16	77,52666667
4	2	515,0266667
5	4	265,0266667
		1332,077778

As it can be seen in Table 6, the time to find the optimal stimulation frequency using the Ternary Search algorithm is about 1.33 seconds. In this way, the use of Ternary Search allows finding the optimal frequency of stimulation during one inhalation (exhalation) by the patient.

There are several other search algorithms, such as *Interpolation Exponential* or *Fibonacci search*. However, their applications are based on the fact that the element being searched for is known. In our case, the optimal frequency of the electrical signal for stimulation is unknown.

Table 7 summarizes the results of the above research.

Table 7. Total time spent on examining one point on a surgical wound using different algorithms on step 6.

N	Algorithms	Ms
1	Linear Search	3612,766324
2	Binary Search	1640,16
3	Jump Search	2778,097143
4	Ternary Search	1332,077778

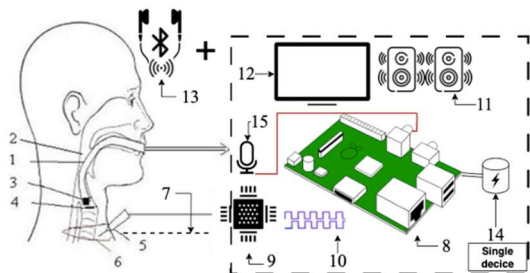
As it is shown in Table 7, the total time spent on examining one point on a surgical wound, which is associated with delays in the functioning of the electrical and electronic part of the device, is acceptable only in the case of applying one of the two algorithms in step 6: *Binary* and *Ternary search*.

Based on the conducted research, an improved algorithm of automatic adjustment of the electrical signal parameters was implemented, and a new version of tools and methods for identification of the recurrent laryngeal nerve during thyroid surgery with automatic adjustment of the electrical signal parameters was developed.

VI. HARDWARE ARCHITECTURE

The new architecture is based on the previously developed architecture and is improved in such a way as to minimize the number of hardware components. This made it possible to develop the complex as a single "single box" device. Schematically, the architecture is shown in Fig. 5.

The proposed architecture makes it possible to remove the main drawback of the previous architecture - an additional visualization unit. Now it is placed in the middle of the case and is a single device. In addition, an internal audio notification unit has been added as part of the device. All this allows using the hardware as a single device. It is worth noting that the connection between the part that controls the process of generating electric pulses and the part that is responsible for processing the information signal is implemented at the software level.



1) breathing tube, 2) larynx, 3) sound sensor, 4) vocal cords, 5) active probe, 6) surgical wound 7) passive probe 8) Raspberry Pi single-board computer, 9) analog circuit 10) rectangular pulses generated by Raspberry Pi 11) internal unit of audio informing surgeon (internal speakers) 12) unit of a visual informing surgeon (screen) 13) external unit of audio informing surgeon (Bluetooth headphones) 14) power supply unit 15) microphone

Figure 5. Schematic representation of the hardware architecture of the rectangle laryngeal nerve identification complex.

Table 8 shows the hardware specification of the device.

Table 8. Specification of the hardware components of the device for identification of RLN

№	Type of component	Name
1	Single-board computer	Raspberry Pi 4 Model B 8GB
2	Screen	7inch LCD 800x480 DSI Touch Screen
3	Cooling system	Active cooling system Raspberry Pi 4B/3B+/3B (19254)
4	Sound card	BauTech CM108 USB
5	Storage	SanDisk microSDHC 32GB Extreme Pro A1 C10 V30 U3 100MB/s
6	Speakers	80mh 5W Speaker + USB Sound Card
7	Microphone	2E Maono ML020
8	Audio receiver/transmitter	VIKEFON KN321
9	Case	SmartPi Touch 2 + Z5B PS 200x90x49
10	Power supply	Power supply Raspberry Pi 4 Model B

A schematic representation of the implementation of hardware components is shown in Fig. 6.



1) Raspberry Pi-4 single-board computer, 2) screen, 3) cooling system, 4) sound card, 5) storage, 6) speakers, 7) microphone, 8) audio receiver/transmitter, 9) case, 10) power supply

Figure 6. Schematic representation of the implementation of the components of the hardware part of the device for the identification of RLN with the algorithm of automatic adjustment of the electrical signal parameters.

The device for identifying the recurrent laryngeal nerve is an autonomous device and operates under the control of the developed software.

VII. SOFTWARE ARCHITECTURE

In previous architecture separate process runs subprocess and communicates with the main application via the Redis database. The program's main process is responsible for monitoring changes in Redis and restarting the pulse generator subprocess whenever there are changes [9]. This architecture uses communication between processes by means of the Redis database [25]. This led to an increase in time spent when examining points on the surgical wound. Long-time delays when changing the frequency can lead to incorrect work of the advanced algorithm for setting the electric current parameters, so they should be minimized. In the improved architecture of software, communication between the function of changing the stimulation frequency and the function of generating rectangular pulses is provided by using stdin/stdout for Inter-Process Communication (IPC) between piped processes [26, 27]. This allows minimizing time delays when changing the stimulation frequency. The improved software architecture of the device for identification of the recurrent laryngeal nerve during thyroid surgery with automatic adjustment of electrical signal parameters is shown in Fig. 7.

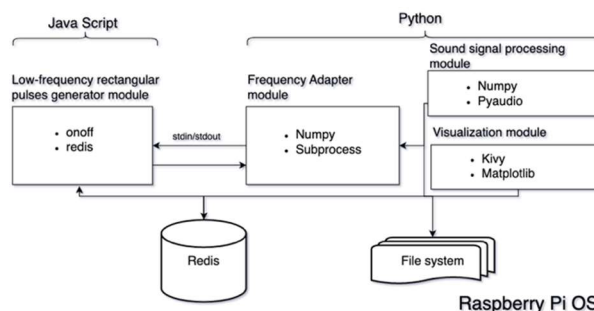


Figure 7. Software architecture of the device for identification of the recurrent laryngeal nerve.

The software runs on the CPU Quad-core Cortex-A72 (ARM v8) 1.5 GHz [28, 29] on a single-board computer Raspberry Pi 4 Model B, operated by Raspberry Pi OS, a Debian-based operating system [30]. The main programming language is Python. In addition, the operating system Raspberry Pi OS is optimized for software in this language.

The main libraries used in software development are as follows. **Kivy** – is an open source software library for developing desktop applications on different platforms [31]. **Numpy** – is a library that provides tools for working with a multidimensional array object [32]. **Matplotlib** – is a comprehensive library for creating static, animated, and interactive visualizations [33]. **Pyaudio** – provides Python bindings for PortAudio v19, the cross-platform audio I/O library [34]. **Subprocess** – provides the ability to manage subprocesses on Python [35, 36].

The main program is built as a desktop app based on the Kivy library. The architecture is based on OOP (object-oriented programming) in combination with EDA [37] (event-driven architecture). Communication between the part responsible for generating rectangular pulses and the part responsible for processing the information signal provided by using stdin/stdout for Inter-Process Communication (IPC) between piped processes. All modules are divided into the following types:

utils – implements the business logic of the application, designed to process simple data;

widgets – the smallest particles of data visualization, responsible for the UI fragment;
screens – application screens, combine widgets, and organize them in a certain order;

configs – static information about the application - setting dictionaries, etc.

The diagram of classes (modules) of the designed software is shown in Fig. 8.

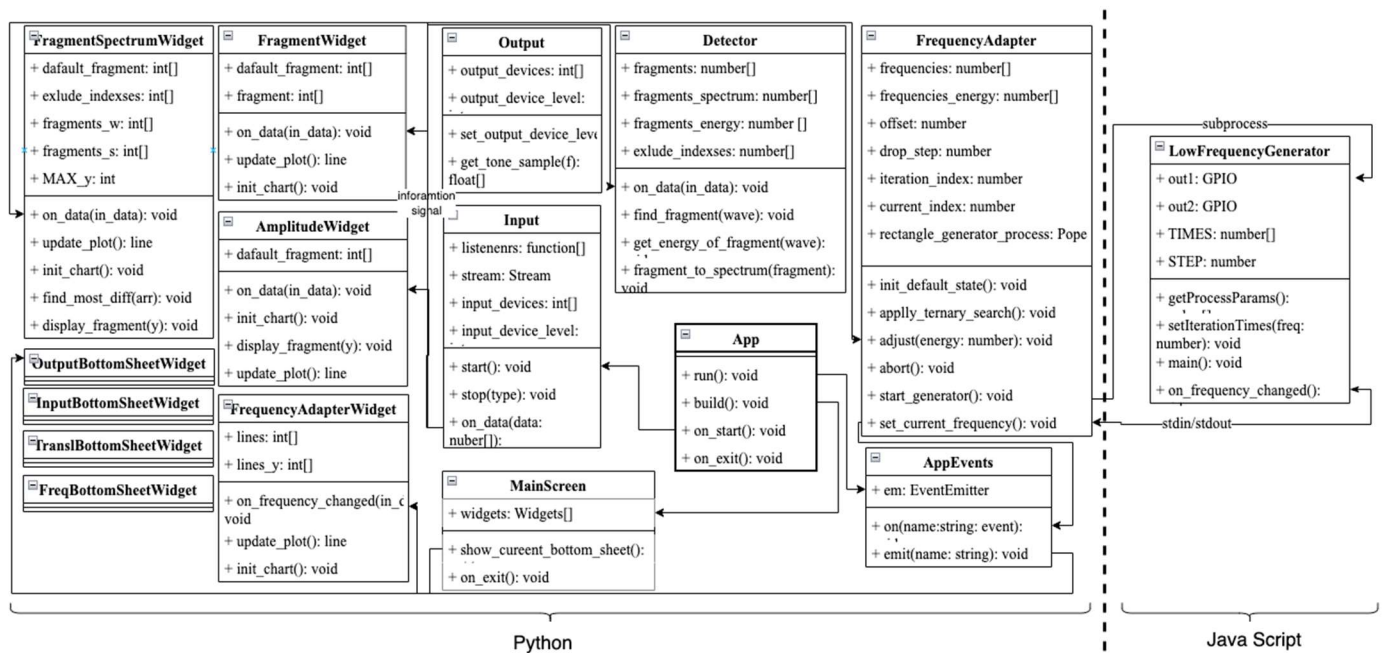


Figure 8. The diagram of classes of the designed software.

The entry point in the application is the **App** module. Communication between modules is based on the **event_emitter** package using the **AppEvent** module, which is a list of all application events. It starts the program and organizes the work of all other modules.

The **LowFrequencyGenerator** module is responsible for generating rectangular pulses. This module is developed using Node and runs as a separate process so as not to block the main process. The **FrequencyAdapter** module is responsible for its launch and maintenance. It also implements the function of controlling the process of automatic adjustment of an electric signal. Communication between these two modules is based on the IPC principle.

MainScreen – responsible for displaying the main screen and placing all other UI modules on the screen. UI modules have the prefix **Widget** in their name and are mainly responsible for displaying information in one form or another.

The **Input** module is designed to read an information signal from a sound card. It is based on the Pyaudio library. After processing the information signal, this module performs the function of presenting the result graphically on the corresponding widgets.

The **Output** module is designed to present the result of classification in the sound form.

The **Detector** module performs the functions of classifying the tissue of a surgical wound at the point of stimulation by electric current. Also, this module communicates with the **FrequencyAdapter** to provide feedback between the parts that are responsible for generating rectangular pulses and information signal processing. This makes it possible to realize the adjustment of an electric signal to the physiological features of the tissues of the surgical wound.

The **AppConfig** module is responsible for storing all

application settings. All settings are written to the file system. This is done so that the next time the application is launched, all settings are saved and applied immediately. Also, this module is responsible for saving settings to the Redis database for communication with other procedures.

The **AmplitudeWidget** module performs the functions of a graphical display of the change in the amplitude of the sound signal in time as the reaction to the stimulation of the tissues of the surgical wound. With the help of the Matplotlib library, a graph of the change in the amplitude of the sound signal depending on time is constructed. To display these changes in real-time, we use the Kivy library Clock to create an interval with which we update the graph at certain time intervals. The **Fragment** and **FragmentSpectrum** modules use a similar mechanism to update their graphs.

The **FragmentWidget** module is responsible for displaying a fragment of the change in the amplitude of the sound signal during the current inhalation (exhalation) by the patient. For this, the plot graph of the Matplotlib library was used.

The **FragmentSpectrumWidget** module performs the function of displaying the spectrum of a fragment of an information signal during the current inhalation (exhalation) by the patient.

The **InputBottomSheetWidget** and **OutputBottomSheetWidget** modules allow to configure the sound card, microphone, and speakers. The **FreqBottomSheetWidget** module is responsible for controlling the frequency of the generation of electric pulses, and the **TransBottomSheetWidget** module - for language selection of the application interface.

The **FrequencyAdapterWidget** module performs functions of visualization of the change in the frequency of generation of rectangular pulses in real-time. Also, the

Matplotlib libraries are used for plotting.

The pm2 library is used for automatic start-up when the device is started. PM2 is a daemon process manager that helps manage and keep applications online 24/7 [37]. First, access to the Redis database and the subprogram for generating rectangular pulses is initialized. After that, the main program starts. In addition to automatic start-up, manual start-up is also possible. For this, a desktop launcher was developed for the Raspbian operating system.

VIII. SOFTWARE FOR ALGORITHM OF AUTOMATIC ADJUSTMENT OF THE ELECTRICAL SIGNAL PARAMETERS

The Ternary Search algorithm is taken to implement the algorithm for automatic adjustment of the electrical signal parameters, as the best of the ones discussed above. Let us consider this algorithm in more detail. Fig. 9 illustrates the basic principle of finding the optimal frequency of an electrical signal for the stimulation of the tissues of a surgical wound. The first step is to divide the range of optimal frequencies of electrical impulses into three sub-ranges that are as equal as possible. Next, the tissue of the surgical wound is stimulated with electrical signals based on frequently selected from each sub-range. Then three information signals obtained as a result of a series of stimulations are processed and we determine the range where the largest amplitude value has been found among the three values of the maximum spectral components of the information signals. In the last step, we conduct stimulation with an electric pulse signal with frequencies from the selected range and determine the frequency of the signal, where there is the greatest response to stimulation.

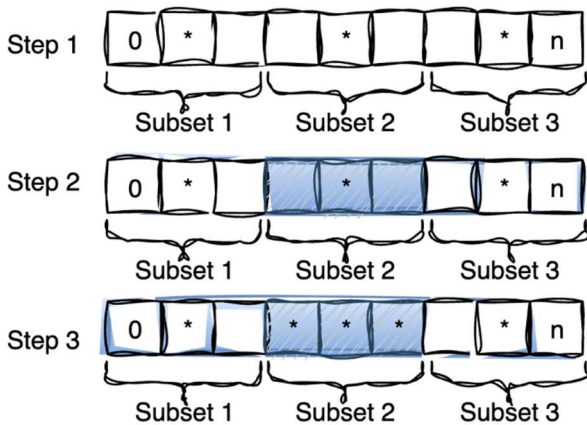


Figure 9. Illustration of adaptation Ternary Search algorithm to find the optimal frequency of the electrical signal.

Applying the algorithm described above, finding the optimal frequency of RLN stimulation in the frequency range of 1-20 Hz can be reduced to 5-6 iterations.

The software implementation of Ternary Search for finding the optimal frequency of stimulation of surgical wound tissues is a loop. At each iteration of it we save the received amplitude of the main spectral component of the information signal for each frequency and *offset*. The offset value indicates in which of the sub-ranges the current frequency of the electrical stimulation signal is located (marks as *current_index*). The algorithm of the method is shown in Fig. 10.

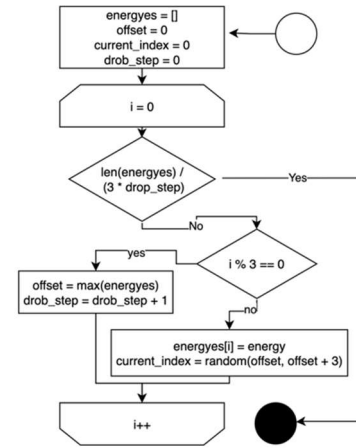


Figure 10. Flow chart of algorithm Ternary Search for finding the optimal frequency of the electrical signal.

The loop ends when the subranges cannot be divided into smaller ones. The developed algorithm is implemented in the *apply_ternary_search* method of the FrequencyAdapter module. It is worth noting that the loop described above is performed with time delays. Each new iteration starts with a delay equal to the time spent on stimulation of the tissue of the surgical wound. For example, if the current frequency of the electrical signal is 4 Hz, then the next iteration starts after 250 ms. The *adjust* method of the FrequencyAdapter module is responsible for starting each iteration at the appropriate time. With each change in the frequency of the electrical signal, the FrequencyAdapter module sends a message to the subprocess of generating rectangular pulses, which applies changes on the hardware level. The PIPE module of the subprocess [38] library is used to transmit the message.

To confirm the efficiency of the proposed approach, a series of experiments was conducted, the results of which are illustrated in Fig. 11.

```

-----Start-----
1 [RG_app]-> Set 6Hz (167 ms) on 47m:12s:849ms - last changes:0ms
2 [RG_app]-> Set 15Hz (67 ms) on 47m:13s:20ms - last changes:171ms
3 [RG_app]-> Set 16Hz (63 ms) on 47m:13s:95ms - last changes:75ms
[RG_app]-> Set 13Hz (77 ms) on 47m:13s:158ms - last changes:63ms
[RG_app]-> Set 15Hz (67 ms) on 47m:13s:244ms - last changes:96ms
[RG_app]-> Set 20Hz (50 ms) on 47m:13s:315ms - last changes:71ms
[RG_app]-> Set 13Hz (77 ms) on 47m:13s:393ms - last changes:78ms
[RG_app]-> adjusting time 545ms ← 6
[RG_app]-> Set 13Hz (77 ms) on 47m:13s:479ms - last changes:0ms
[RG_app]-> Set 13Hz (77 ms) on 47m:13s:564ms - last changes:0ms
[RG_app]-> Set 13Hz (77 ms) on 47m:13s:649ms - last changes:0ms
[RG_app]-> Set 13Hz (77 ms) on 47m:13s:735ms - last changes:0ms
[RG_app]-> Set 13Hz (77 ms) on 47m:13s:826ms - last changes:0ms
[RG_app]-> Set 13Hz (77 ms) on 47m:13s:905ms - last changes:0ms
[RG_app]-> Set 13Hz (77 ms) on 47m:14s:2ms - last changes:0ms
[RG_app]-> Set 13Hz (77 ms) on 47m:14s:87ms - last changes:0ms
[RG_app]-> Set 13Hz (77 ms) on 47m:14s:172ms - last changes:0ms
[RG_app]-> Set 13Hz (77 ms) on 47m:14s:268ms - last changes:0ms
[RG_app]-> Set 13Hz (77 ms) on 47m:14s:353ms - last changes:0ms
[RG_app]-> Set 13Hz (77 ms) on 47m:14s:434ms - last changes:0ms
[RG_app]-> Set 13Hz (77 ms) on 47m:14s:524ms - last changes:0ms
[RG_app]-> Set 13Hz (77 ms) on 47m:14s:617ms - last changes:0ms
[RG_app]-> fragment time 1769ms ← 7
-----End-----

```

1) the current iteration of the Ternary Search loop; 2) the predicted iteration duration; 3) the current stimulation frequency for the current iteration; 4) the current execution time; 5) the duration of the previous iteration; 6) the total duration of automatic adjustment of the electrical signal; 7) the total duration of the information signal fragment

Figure 11. The result of the application software for automatic adjustment of electrical signal.

As it can be seen in Fig. 11, for each iteration of the Ternary Search loop (1), the current stimulation frequency for the current iteration (3), the predicted duration of the iteration at this frequency (2), and the current execution time (4) are shown. Measurements were made for the duration of each iteration (5). As it is shown in Fig. 11, the actual and predicted times are almost identical. The total duration of the automatic adjustment of the electrical signal loop was also measured (6). As it is shown, the duration was **545 ms**, while the duration of the information signal fragment (patient inhalation) (7) was **1769 ms**. This means that during **1224 ms** of the duration of the patient's inhalation, the tissues of the surgical wound are stimulated with an optimal frequency.

IX. THE RESULT OF THE APPLICATION SOFTWARE FOR AUTOMATIC ADJUSTMENT OF ELECTRICAL SIGNAL

Fig. 12 shows an image of the developed device for identifying the recurrent laryngeal nerve with the function of the automatic adjustment of an electric signal.



Figure 12. The device for identifying the recurrent laryngeal nerve with the function of automatic adjustment of an electrical signal.

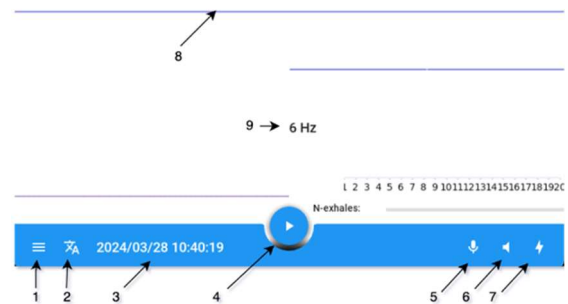
Let us consider the abilities of the software:

- Generation of rectangular pulses.
- Controlling the process of automatic adjustment of an electrical signal
 - Getting the information signal from the microphone
 - The output of the information signal from the microphone to the sound device (both external - headphones and internal - speakers)
 - Visualization: information signal amplitudes; information signal fragment; fragment of the information signal in spectral form; changes in the frequency of generation of rectangular pulses in real-time.
 - Classification of surgical wound tissues, visual and audio information about the appropriate type.
 - Localization of the application (changing the language of the interface)
 - Setting the stimulation frequency manual (as an additional option).
 - Autostart by turning on the device.

The software of the device is a desktop application. It starts when the device starts. The home screen has three main areas

and controls at the bottom of the screen. The control panel contains a button to start recording, elements for selecting a microphone, and speakers.

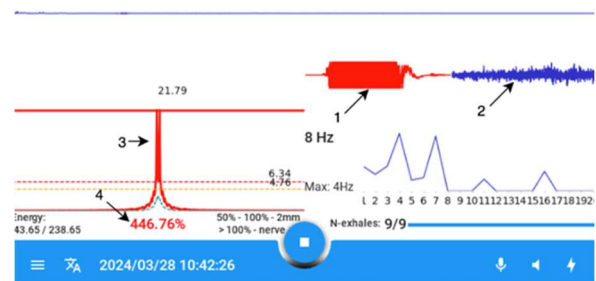
Figures 13-15 show the elements of the graphic interface of the developed device.



1) navigation menu, 2) localization menu, 3) current date, 4) start recording button, 5) microphone settings menu, 6) speaker settings menu, 7) rectangular pulse generation settings menu, 8) visual representation of the information signal, 9) frequency of generation of rectangular pulses

Figure 13. The main screen of the application.

To start work, it is needed to press the start recording button (1). The application will start recording and displaying the results on the screen and speakers. At the top of the screen, there is a visualization of the sound wave of the information signal (8). Information about the frequency of generation of rectangular pulses is also displayed on the main screen (9).



1) fragment of the information signal (segment of type 1, Fig. 2) 2) segment of type 2 (Fig. 2), 3) spectrum of the information signal 4) calculated energy of the fragment of the information signal

Figure 14. The main screen of the application in the mode of stimulating the tissue of a surgical wound.

The software also allows one to choose the source of the sound signal reading and adjust its sensitivity. Choosing the source of the output of the surgical wound tissue classification result (speakers, headphones) and adjusting their volume, is also possible. The rectangular pulse generation settings menu provides an opportunity to disable the automatic generation frequency adjustment algorithm. In this case, it is possible to manually adjust the desired frequency. The localization menu allows selection the language of the interface. After selecting the language, the interface will be changed immediately without the need to restart the application. The screen forms of the above settings are shown in Fig. 15.



1) the microphone setting screen form; 2) the screen form for setting speakers; 3) the screen form for localization of application; 4) the screen form for setting the frequency of generation of rectangular pulses;

Figure 15. Screen forms for configuring the application.

It should also be added that it would be advisable to look for an area where the RLN is guaranteed to be. It is possible to use the algorithm from work [38] for this. In conclusion, it should be noted that one of the complex stages of information signal processing is its segmentation (Step 3). In further studies, this stage is expected to be carried out on the basis of neural networks [39-42].

X. CONCLUSIONS

Methods and tools for identifying the recurrent laryngeal nerve during surgery on the thyroid gland are considered. In the developed device, for the first time, the method and software of adjusting the parameters of the electrical signal, with the mean of the tissues of the patient's surgical wound stimulated, is implemented. Research on the time characteristics of the process of adjusting the electrical signal parameters was conducted. It was found that in the known method of adjusting the parameters, the total time spent on examining one point on the surgical wound is associated with delays in the functioning of the electrical and electronic parts of the device. These delays do not make it possible to implement this procedure of adjusting during one stimulation. For the first time, the use of well-known methods for sorting elements of the Ternary search array was proposed and substantiated for setting the frequency of electrical pulses. The use of this sorting method made it possible to achieve an acceptable total time spent on the examination of one point on the surgical wound during the thyroid gland surgery.

The article also presents the hardware and software of the device for identifying the recurrent laryngeal nerve with the function of automatic adjustment of an electric signal. In the mentioned device, the function of adjusting the parameters of the electrical signal, which stimulates the tissues of the surgical wound, is implemented according to the individual electrophysiological properties of the tissues of the patient's surgical wound. The improved hardware architecture made it possible to create a complex in the form of "one box". This simplified its use during operations on the thyroid gland a lot.

The updated architecture of the software is presented, which implements communication between the function of changing the stimulation frequency and the function of generating rectangular pulses based on principles of Inter-Process Communication (IPC) between piped processes. The latter made it possible to avoid time delays when changing the frequency of the electrical signal that stimulates the tissues. The software of the algorithm for automatic adjustment of the electrical signal parameters is presented.

Validation of hardware and software complex for

identifying the recurrent laryngeal nerve with the function of automatic adjustment of an electrical signal at the VITASANA Medical Center in the city of Ternopil remains one of the main tasks related to developing this work.

References

- [1] G. Gremillion, A. Fatakia, A. Dornelles, R. G. Amedee, "Intraoperative recurrent laryngeal nerve monitoring in thyroid surgery: is it worth the cost?," *Ochsner J.*, vol. 12, issue 4, pp. 363-366, 2012. PMID: 23267265; PMCID: PMC3527866.
- [2] G. Dionigi, C. W. Wu, H. Y. Kim, S. Rausei, L. Boni, F. Y. Chiang, "Severity of recurrent laryngeal nerve injuries in thyroid surgery," *World J Surg.*, vol. 40, issue 6, pp. 1373-1381, 2016. <https://doi.org/10.1007/s00268-016-3415-3>. PMID:26817650.
- [3] P. Mattsson, J. Hydman, M. Svensson, "Recovery of laryngeal function after intraoperative injury to the recurrent laryngeal nerve," *Gland Surg.*, vol. 4, issue 1, pp. 27-35, 2015. <https://doi.org/10.3978/j.issn.2227-684x.2015.01.10>. PMID: 25713777; PMCID: PMC4321052.
- [4] J. I. Staubitz, F. Watzka, A. Poplawski, P. Riss, T. Clerici, A. Bergenfelz, T. J. Musholt & EUROCRINE® Council, "Effect of intraoperative nerve monitoring on postoperative vocal cord palsy rates after thyroidectomy: European multicentre registry-based study," *BJS Open*, vol. 4, issue 5, pp. 821-829, 2020. <https://doi.org/10.1002/bjs.5.50310>. Epub 2020 Jun 16. PMID: 32543773; PMCID: PMC7528513.
- [5] W. Liddy, B. R. Lawson, S. R. Barber, D. Kamani, M. Shama, S. Soyly, C. W. Wu, F. Y. Chiang, J. Scharpf, M. Barczynski, H. Dralle, S. Van Slycke, R. Schneider, G. Dionigi, G. W. Randolph, "Anterior laryngeal electrodes for recurrent laryngeal nerve monitoring during thyroid and parathyroid surgery: New expanded options for neural monitoring," *Laryngoscope*, vol. 128, issue 12, pp. 2910-2915, 2018. <https://doi.org/10.1002/lary.27362>. PMID:30417384.
- [6] F.-F. Chou, C.-M. Hsu, C.-C. Lai, Y.-C. Chan, S.-Y. Chi, "Bilateral vocal cord palsy after total thyroidectomy – A new treatment – Case reports," *International Journal of Surgery Case Reports*, vol. 38, pp. 32-36, 2017. <https://doi.org/10.1016/j.ijscr.2017.06.045>. PMID:28734186 PMCID:PMC5521027
- [7] A. Kurz, et al., "Comparison of voice therapy and selective electrical stimulation of the larynx in early unilateral vocal fold paralysis after thyroid surgery: A retrospective data analysis," *Clinical Otolaryngology*, vol. 46, issue 3, pp. 530-537, 2021. <https://doi.org/10.1111/coa.13703>. PMID:33370506 PMCID:PMC8048835
- [8] G. Alon, "Functional Electrical Stimulation (FES): Transforming clinical trials to neuro-rehabilitation clinical practice – A forward perspective," *Journal of Novel Physiotherapies*, vol. 3, issue 5, 1000176, 2013. <https://doi.org/10.4172/2165-7025.1000176>.
- [9] A. Dyvak, V. Tymets, "An improved method and means with the function of automatic adjustment of electrical signal parameters for detection of the recurrent laryngeal nerve," *Computational Problems of Electrical Engineering*, vol. 13, no. 2, pp. 1-8, 2023. <https://doi.org/10.23939/jceee2023.02.001>.
- [10] J. Y. Chen, Q. Shen, "A new technique for identifying the recurrent laryngeal nerve: Our experience in 71 patients," *Chin Med J (Engl)*, vol. 131, issue 7, pp. 871-872, 2018. <https://doi.org/10.4103/0366-6999.228241>. PMID:29578136 PMCID:PMC5887751.
- [11] N. Ocheretnyuk, I. Voytyuk, M. Dyvak and Y. Martsenyuk, "Features of structure identification the macromodels for nonstationary fields of air pollutions from vehicles," *Proceedings of International Conference on Modern Problem of Radio Engineering, Telecommunications and Computer Science*, Lviv, Ukraine, 2012, pp. 444.
- [12] M. Dyvak, "Parameters identification method of interval discrete dynamic models of air pollution based on artificial bee colony algorithm," *Proceedings of the 2020 10th International Conference on Advanced Computer Information Technologies (ACIT)*, Deggendorf, Germany, 2020, pp. 130-135, <https://doi.org/10.1109/ACIT49673.2020.9208972>.
- [13] B. C. Tsui, "Electrical impedance to distinguish intraneural from extraneural needle placement in porcine nerves during direct exposure and ultrasound guidance," *Anesthesiology*, vol. 109, pp. 479-483, 2008. <https://doi.org/10.1097/ALN.0b013e318182c288>. PMID:18719446.
- [14] K. E. Barrett, S. M. Barman, S. Boitano, H. Brooks, *Ganong's Review of Medical Physiology*, (24 ed.), 2012, 619 p. ISBN 978-0071780032.
- [15] M. Dyvak, A. Pukas, I. Oliynyk and A. Melnyk, "Selection the "Saturated" block from interval system of linear algebraic equations for recurrent laryngeal nerve identification," *Proceedings of the IEEE Second International Conference on Data Stream Mining & Processing (DSMP)*, Lviv, Ukraine, pp. 444-448, 2018. <https://doi.org/10.1109/DSMP.2018.8478528>.

- [16] P. Duhamel, M. Pierre, "Fast Fourier transforms: a tutorial review and a state of the art," *Signal Processing*, vol. 19, issue 4, pp. 259–299, 1990. [https://doi.org/10.1016/0165-1684\(90\)90158-U](https://doi.org/10.1016/0165-1684(90)90158-U).
- [17] A. Edelman, P. McCorquodale, S. Toledo, "The future fast Fourier transform?," *SIAM Journal on Scientific Computing*, vol. 20, issue 3, 1094–1114, 1998. <https://doi.org/10.1137/S1064827597316266>.
- [18] "Complete list of C/C++ FFT libraries," *VCV Community*, 2020. Retrieved 2021-03-03.
- [19] P. H. Charlton, D. A. Birrenkott, T. Bonnici, M. A. Pimentel, A. E. Johnson, J. Alastruey, et al., "Breathing rate estimation from the electrocardiogram and photoplethysmogram: A review," *IEEE Reviews in Biomedical Engineering*, vol. 11, pp. 2–20, 2018. <https://doi.org/10.1109/RBME.2017.2763681>. PMID:29990026 PMCid:PMC7612521.
- [20] D. R. Hillman, P. R. Platt, P. R. Eastwood, "The upper airway during anaesthesia," *Br J Anaesth*, vol. 91, issue 1, pp. 31-39, 2003. <https://doi.org/10.1093/bja/aeg126>. PMID:12821563.
- [21] Linear Search – Data Structure and Algorithm Tutorials. [Online]. Available at: <https://www.geeksforgeeks.org/linear-search/>
- [22] Binary Search – Data Structure and Algorithm Tutorials. [Online]. Available at: <https://www.geeksforgeeks.org/binary-search/>
- [23] Jump Search – Data Structure and Algorithm Tutorials. [Online]. Available at: <https://www.geeksforgeeks.org/jump-search/>
- [24] Ternary Search – Data Structure and Algorithm Tutorials. [Online]. Available at: <https://www.geeksforgeeks.org/ternary-search/>
- [25] L. Fugaro, M. Ortensi, *Redis Stack for Application Modernization: Build real-time multi-model applications at any scale with Redis*, Kindle Edition, Packt Publishing, 1st edition, 2023, ASIN:B0CMR28RT1.
- [26] Inter Process Communication. [Online]. Available at: <https://www.geeksforgeeks.org/inter-process-communication-ipc/>
- [27] J. S. Gray, *Interprocess Communications in Linux: The Nooks and Crannies*, 1st Edition, Prentice Hall, 2003, ISBN-13:978-0130460424.
- [28] Raspberry Pi 4 Model B specifications – Raspberry Pi. [Online]. Available at: <https://www.raspberrypi.com/products/raspberry-pi-4-model-b/specifications/>
- [29] Raspberry Pi Documentation - BCM2711 [Online]. Available at: <https://www.raspberrypi.com/documentation/computers/processors.html#bcm2711>
- [30] STM32 GPIO Lecture 15: GPIO output speed register and its applicability. [Online]. Available at: <https://fastbitlab.com/gpio-output-speed-register-applicability/#:~:text=If%20you%20select%20GPIO%20pin,speed%20frequency%20up%20to%20100MHz.>
- [31] Kivy documentation. [Online]. Available at: <https://kivy.org/doc/stable/>
- [32] Numpy documentation. [Online]. Available at: <https://numpy.org/doc/stable/>
- [33] Matplotlib. [Online]. Available at: <https://matplotlib.org/stable/>
- [34] Pyaudio. [Online]. Available at: <https://people.csail.mit.edu/hubert/pyaudio/>
- [35] Subprocess – Subprocess management – Python 3.12.4 documentation [Online]. Available at: <https://docs.python.org/3/library/subprocess.html>
- [36] M. Stack, *Event-Driven Architecture in Golang Building Complex Systems with Asynchronicity and Eventual Consistency*, Packt Publishing, 2022, ISBN:9781803232188.
- [37] PM2 – Single Page Doc [Online]. Available at: <https://pm2.keymetrics.io/docs/usage/pm2-doc-single-page/>
- [38] M. Dyvak, P. Stakhiv, A. Pukas, "Algorithms of parallel calculations in task of tolerance ellipsoidal estimation of interval model parameters," *Bulletin of the Polish Academy of Sciences-Technical Sciences*, vol. 60, issue 1, pp. 159-164, 2012. <https://doi.org/10.2478/v10175-012-0022-9>.
- [39] N. Lutsiv, T. Maksymyuk, M. Beshley, O. Lavriv, V. Andrushchak, et al., "Deep semisupervised learning-based network anomaly detection in heterogeneous information systems," *Computers, Materials & Continua*, vol. 70, issue 1, pp. 413-431. <https://doi.org/10.32604/cmc.2022.018773>.
- [40] A. Sachenko, V. Kochan, V. Turchenko, V. Tymchysyn, N. Vasylykiv, "Intelligent nodes for distributed sensor network," *Proceedings of the 16th IEEE Instrumentation and Measurement Technology Conference (IMTC/99)*, Venice, Italy, 24–26 May 1999, pp. 1479–1484. <https://doi.org/10.1109/IMTC.1999.776072>.
- [41] E. Kariri, H. Louati, A. Louati, F. Masmoudi, "Exploring the advancements and future research directions of artificial neural networks: A text mining approach," *Appl. Sci.*, vol. 13, 3186, 2023. <https://doi.org/10.3390/app13053186>.
- [42] I. Paliy, A. Sachenko, V. Koval and Y. Kurylyak, "Approach to face recognition using neural networks," *Proceedings of the 2005 IEEE Intelligent Data Acquisition and Advanced Computing Systems: Technology and Applications (IDAACS'2005)*, Sofia, Bulgaria, 2005, pp. 112-115, <https://doi.org/10.1109/IDAACS.2005.282951>.



MYKOLA DYVAK, a Professor, Vice-Rector for Research of West Ukrainian National University. Research interests: *Mathematical modeling of static, dynamic systems and systems with distributed parameters, Structural and parametric identification of systems, Calculation methods, Parallelization of calculations for interval analysis tasks, Interval data analysis, Application of interval methods in environmental monitoring and for modeling distributed systems.*



Volodymyr TYMETS, PhD, a senior researcher of West Ukrainian National University. Research interests: *method of recurrent laryngeal nerve recognition during thyroid surgery, information technologies, computer science.*



Andriy DYVAK, PhD student of West Ukrainian National University. Now he works as a surgeon in the clinical hospital in Ternopil. Research areas: *information technologies, medical systems, mathematical models, computer science.*

...